Supplementary Information (SI) for Chemical Science.

Supporting Information

Electrochemical Ammonia Oxidation with a Homogeneous Molecular Redox Mediator

Tarisha Gupta,*[a] Sanyam,[a] Shivani Saraswat,[a] Anirban Mondal,*[a] Biswajit Mondal*[a]

Department of Chemistry, Indian Institute of Technology Gandhinagar, Palaj, Gujarat, India-382055

Corresponding authors E-mail: tarishag@iitgn.ac.in, amondal@iitgn.ac.in and mondal.biswajit@iitgn.ac.in

Experimental Procedures

1.1 Materials and Methods

All the reagents were purchased from commercial sources and used without further purification. Chloroform-D ($CDCl_3$, 99.8 atom% D) was procured from Sigma-Aldrich. Ferrocenecarboxylic acid (97%) and sulfanilamide were purchased from BLD Pharm, India. Ammonia solution (30%) was purchased from Merck Life Science *Pvt. Ltd.*, India. Triethylamine (Et_3N, 98%), 2-aminopyridine (98%), and molecular sieves (3 and 4 Å) were purchased from Avra Synthesis *Pvt. Ltd.*, India. Tetrabutylammonium tetrafluoroborate (TBAF, > 98%), Acetonitrile-D_3 (CD_3CN, 99.8 atom% D), 1-Naphthylamine, Vanadium (III) Chloride (VCl_3), and Ferrocene (Fc, > 98%) were obtained from TCI chemicals. Dichloromethane (DCM, AR dry solvent), *N, N*-Dimethylformamide (DMF, AR dry solvent), Ethyl acetate, Dry dimethyl sulfoxide (AR dry DMSO) and Dry Acetonitrile (AR dry solvent), pyridine (py), and sodium sulfate anhydrous (Na_2SO_4, 99%) were purchased from Finar, India. Aniline (99%), Hexafluorophosphate Azabenzotriazole Tetramethyl Uronium (HATU, 98%), Oxalyl chloride {$(COCl)_2$, 97.5%}, *N, N*-Diisopropylethylamine (DIPEA, 98%), and 2-amino-6-methylpyridine (98%) were procured from Loba Chemie *Pvt. Ltd*., India. Dimethyl sulfoxide (DMSO-d_6) was purchased from Eurisotop. *N*-pyridylferrocenecarboxamide (Fcpy), *N*-phenylferrocenecarboxamide (FcPh) and *N*-(6-methylpyridin-2-yl)ferrocenecarboxamide, ($Fcpy_{Me}$) were prepared using the following reported methods.[1]

^{1}H-NMR spectra were recorded on a Bruker Avance III 500 MHz and Jeol JNM-ECZL S, 400 MHz spectrometer. The Shimadzu UV-3600 I Plus spectrophotometer was used for UV-Vis spectral studies. The electrode surface characterization was performed by Field Emission Scanning Electron Microscopy (FE-SEM) with Jeol JSM7600F instrument.

1.2 Synthesis and Characterization

The *N*-pyridylferrocenecarboxamide (Fcpy) was synthesized using the reported literature method.[1] First, in a clean and dry round-bottom flask, Ferrocenecarboxylic acid, HATU, and DIPEA were mixed in the equivalent ratio of 1: 1.5: 3 at room temperature. Dry DMF (3 mL) was added as a solvent, and the reaction mixture was kept for stirring at 70℃ for 1 hour under degassed conditions. Formation of orangish brown-coloured intermediate in the first step, and then 2-aminopyridine (1.2 equiv.) was added to the reaction mixture in the second step. The dark-brown colored reaction mixture was kept on stirring for 24 hours under inert conditions. The product was extracted in ethyl acetate and isolated in 3-5% ethyl acetate-hexane through column chromatography. Fcpy (80 mg, 30 %); ^{1}H NMR (500 MHz, $CDCl_3$) δ 8.31 (dd, J = 12.8, 6.5 Hz, 2H), 8.17 (s, 1H), 7.79 – 7.70 (m, 1H), 7.08 – 7.03 (m, 1H), 4.86 – 4.84 (m, 2H), 4.46 – 4.43 (m, 2H), 4.26 (s, 5H). ^{13}C NMR (126 MHz, $CDCl_3$) δ 169.23, 151.59, 147.73, 138.52, 119.48, 113.96, 75.34, 71.33, 69.99, 68.48. ESI-MS calculated for $C_{16}H_{15}FeN_2O$ $(M+H)^+$ 307.05, found 307.05. IR ($\nu_{C=O}$: 1643 cm^{-1} and UV: λ_{max} (MeCN) 442 nm.

1.3 Electrochemical Measurements

All the measurements were performed in a three-electrode system using *CHI 7044E* potentiostat. Ag/AgCl and a Pt wire were used as the pseudo-reference and counter electrodes. A glassy carbon electrode (GCE) was used as a working electrode in all the experiments and polished after each scan. Ferrocene (Fc) was added to the solution at the end of each experiment, and a CV scan was recorded to measure this potential to calibrate the Ag/AgCl potentials *w.r.t.* $Fc^{+/0}$. All CV experiments were conducted at the scan rate of 100 mV s^{-1} unless otherwise mentioned. 100 mM Tetrabutylammonium tetrafluoroborate ($^nBu_4NBF_4$) was used as a supporting electrolyte in all the electrochemical experiments.

For CV experiments, solutions were degassed by purging Ar/N_2 through the solvent for 20 min. In CV experiments, the amount of mediator was taken as 1 mM with saturated NH_3 from aq. NH_3 solution through Ar/N_2 purging. For electrochemical AOR, saturation of ammonia was done by bubbling 20 mL of aq. NH_3 solution in 4 mL electrolyte containing 100 mM TBAF (supporting electrolyte) for 20 minutes. To determine the concentration of NH_3 in NH_3-saturated MeCN and DMSO, 5 mL of aq. NH_3 solution was bubbled for 5 min into 1 mL CD_3CN/DMSO-d_6 containing 100 mM TBAF (as internal standard).[2] The resultant solution was analyzed using ^{1}H-NMR, and the concentration of saturated NH_3 was assessed *w.r.t.* TBAF concentration. An average of three measurements resulted in an NH_3 concentration of 0.5 M in MeCN and 1.0 M in DMSO.

For the NH_3 concentration dependence study, the calculated amount (in µL) of aqueous ammonia solution was directly added to the acetonitrile to maintain the corresponding concentration (considering 30 % purity of the aqueous ammonia solution). For example, for 10 mM aq. NH_3, the amount added was 5.24 µL, whereas for 100 mM aq. NH_3, it was 52.4 µL. To rule out the role of water in aqueous ammonia solution during the AOR study, similar volumes (taken during the NH_3 concentration dependence experiment) of water were added, resulting in no dependence of water concentration on the reaction rate.

To evaluate the efficiency of Fcpy as a redox mediator for ammonia oxidation, we determined the overpotential for the catalytic process in acetonitrile (MeCN) using homogeneous electrochemical studies. The thermodynamic potential for ammonia oxidation in MeCN has been reported as -0.94 V *vs.* $Fc^{+/0}$.[2–4] From cyclic voltammetry measurements, the onset potential for Fcpy-mediated ammonia oxidation in MeCN is observed at 20 mV *vs.* $Fc^{+/0}$ (**Figure 1a**), measured at the inflection point of catalytic current from the background. The overpotential (η) is calculated as the difference between the thermodynamic potential ($E°$) and the experimentally determined onset potential (E_{onset}):

$$\eta = E_{onset} - E° = 0.020\ \text{V} - (-0.94\ \text{V}) = 0.96\ \text{V}$$

Therefore, the overpotential for Fcpy-mediated ammonia oxidation in MeCN is 960 mV. This value provides a benchmark for evaluating the catalytic performance of Fcpy under thermodynamically relevant conditions.

Bulk electrolysis at constant potential was performed in dry and Ar purged conditions at 0.28 V with and without a mediator (blank) using a large surface area (1*1 cm^2) carbon cloth electrode for 1 h. The amount of mediator has been taken as 1 mM in acetonitrile (4 mL) with 100 mM TBAF as supporting electrolyte and saturated NH_3 from aq. NH_3 solution.

% Faradaic yield (FY) was determined from the following equation:

$$FE\ (\%) = \frac{moles\ of\ product\ formed\ \times 96{,}485\ (C\ mol^{-1})\ \times\ n}{total\ charge\ passed\ (C)} \times 100\ \% \qquad (\textbf{\textit{eq. S1}})$$

where n is the number of electrons involved in the reaction (Here, n = 6)

1.4 Foot-of-the-wave Analysis and Determination of k_{obs}

Foot-of-the-Wave Analysis (FOWA) was employed to extract kinetic parameters from CV experiments. Initially, a cyclic voltammogram was obtained for each mediator in the absence of substrate for the determination of the half-wave potential ($E_{1/2}$) of the mediator and the anodic peak current (i_p^o) values. CV recorded in the presence of substrate (NH_3) gives the catalytic current (*i*) values and has been used for the following **equation S3**:

$$\frac{i}{i^o} = \frac{2.24\, n_{cat}^{\sigma}\sqrt{\dfrac{k_{obs}}{fv}}}{[f(E_{1/2} - E)]} \qquad (\textbf{\textit{eq. S2}})$$

where *E* is the applied potential, ν is the scan rate (V/s), k_{obs} is the observed rate constant, and f = F/RT = 38.94 V^{-1}. n_{cat} is the number of electrons required for catalysis (n_{cat} = 6 in this case). The superscript (σ) depends on the mechanism of electron transfer (here, σ = 1). The plot of *i*/i_p^o versus $[1 + e^{[f(E_{1/2} - E)]}]^{-1}$ estimates the observed rate constant from the slope of the obtained straight line.[5]

1.5 Determination of k_{obs} from CV using peak current method:[6]

$$i_{cat} = n_{cat}FAC_{cat}\sqrt{Dk_{obs}} \qquad (\textbf{\textit{eq. S3}})$$

$$i_p = 0.4463 n_p^{3/2} FAC_{cat}\sqrt{\frac{F}{RT}Dv} \qquad (\textbf{\textit{eq. S4}})$$

$$\frac{i_{cat}}{i_p} = \frac{1}{0.4463} \frac{n_{cat}}{n_p^{3/2}} \sqrt{\frac{RTk_{obs}}{Fv}} \qquad (\textbf{\textit{eq. S5}})$$

The observed catalytic current plateau under NH_3 saturation conditions is described by **equation S3**, which models the steady-state current arising from a diffusion-limited catalytic process. In this expression, n_{cat} (here, 6 for NH_3 to N_2 conversion) represents the number of electrons involved in the catalytic reaction, F is Faraday's constant, A is the geometric area of the working electrode, C_{cat} is the bulk concentration of the catalyst, D is the diffusion coefficient of the catalytically active species, k_{obs} is the apparent rate constant. To quantify catalytic efficiency, the catalytic current (i_{cat}) is normalized to the peak current (i_p) of the non-catalytic redox event in the absence of substrate (**equation S5**). This normalization incorporating parameters such as the number of electrons in the non-catalytic event (n_p = 1), the universal gas constant (R), temperature (T), and the scan rate (v) of the potential sweep.

Using the slope value of i_{cat}/i_p *vs.* $\nu^{-1/2}$ plot from the scan-rate dependent mediated AOR in MeCN, the k_{obs} is calculated as 0.046 ± 0.002 s^{-1}(average of three measurements).

1.6 Product Analysis

(a) Gaseous products: After bulk electrolysis, the amount of produced hydrogen and nitrogen in the reactor headspace was analyzed using a gas chromatograph (CIC-Dhruva) equipped with a thermal conductivity detector (TCD).[7] The moles were calculated according to the literature method reported.[8]

(b) Modified Griess colorimetric method for the detection of nitrite and nitrate: After electrolysis, the electrolyte solution was evaporated, and workup was done using dichloromethane and water. The aqueous layer was collected, and the corresponding volume was noted down (10 mL).

The determination of NO_2^- and NO_3^- ions was done using the modified Griess colorimetric method following the previously reported literature method.[9] For the preparation of the color reagent, 1 mmol (172 mg) of sulfanilamide and 0.5 mmol 130 mg of 1-napthylamine were dissolved in 10 mL of 37% HCl, then diluted to 200 mL with milli-Q water. In the case of the nitrate colorimetric test, an addition of 3 mmol (470 mg) of VCl_3 as a reducing agent was added to convert nitrate to nitrite. The stock solutions of 10 mM sodium nitrite and 10 mM potassium nitrate were used to prepare the standard solutions of 5 μM to 50 μM by dilution using milli-Q water for the calibration of nitrite and nitrate, respectively. In a test tube, the reaction was done using 2 mL of standard $NaNO_2$/ KNO_3 solution of specific concentration with 2 mL of the color reagent on a heating water bath at 50-60 °C for 5 min. For all standard concentrations, the resulting mixture was analyzed with UV-visible spectroscopy, with the absorbance measured at λ_{max} = 518 nm. The calibration was repeated three times, and the averaged calibration data were plotted (separately for nitrite and nitrate) with error bars. In the post-electrolysis analyte solution, nitrite and nitrate concentrations were quantified using a similar procedure using 2 mL of it with 2 mL of respective color reagent and corresponding calibration plot.

NOTE:

1. The color reagents were stored in the dark at refrigerated conditions.
2. The solutions were stored in the dark at refrigerated conditions.
3. VCl_3 is air and light sensitive.

1.7 Computational Estimation of Kinetic Isotope Effect (*KIE*) for the PCET Step

To support the proposed mechanism and specifically the identification of the PCET step as rate-limiting (Step 2), we performed computational calculations to estimate the kinetic isotope effect (*KIE*). All calculations were carried out using the ORCA 5.0 quantum chemistry package.[10] Geometry optimizations and transition state searches were performed at the B3LYP/def2-SVP level of theory. The reaction pathway was explored using the nudged elastic band (NEB) method to locate the transition state structure accurately. Our approach follows the methodology reported by Melander and Saunders.[11,12] The calculated *KIE* (the ratio k_H/k_D) was 1.2, indicating a measurable isotope effect associated with transferring a proton during Step 2. This value is consistent with prior reports for PCET-dominated reaction steps in similar systems.[4] These computational results provide additional support for the mechanistic assignment of Step 2 as the rate-limiting step in the catalytic cycle.

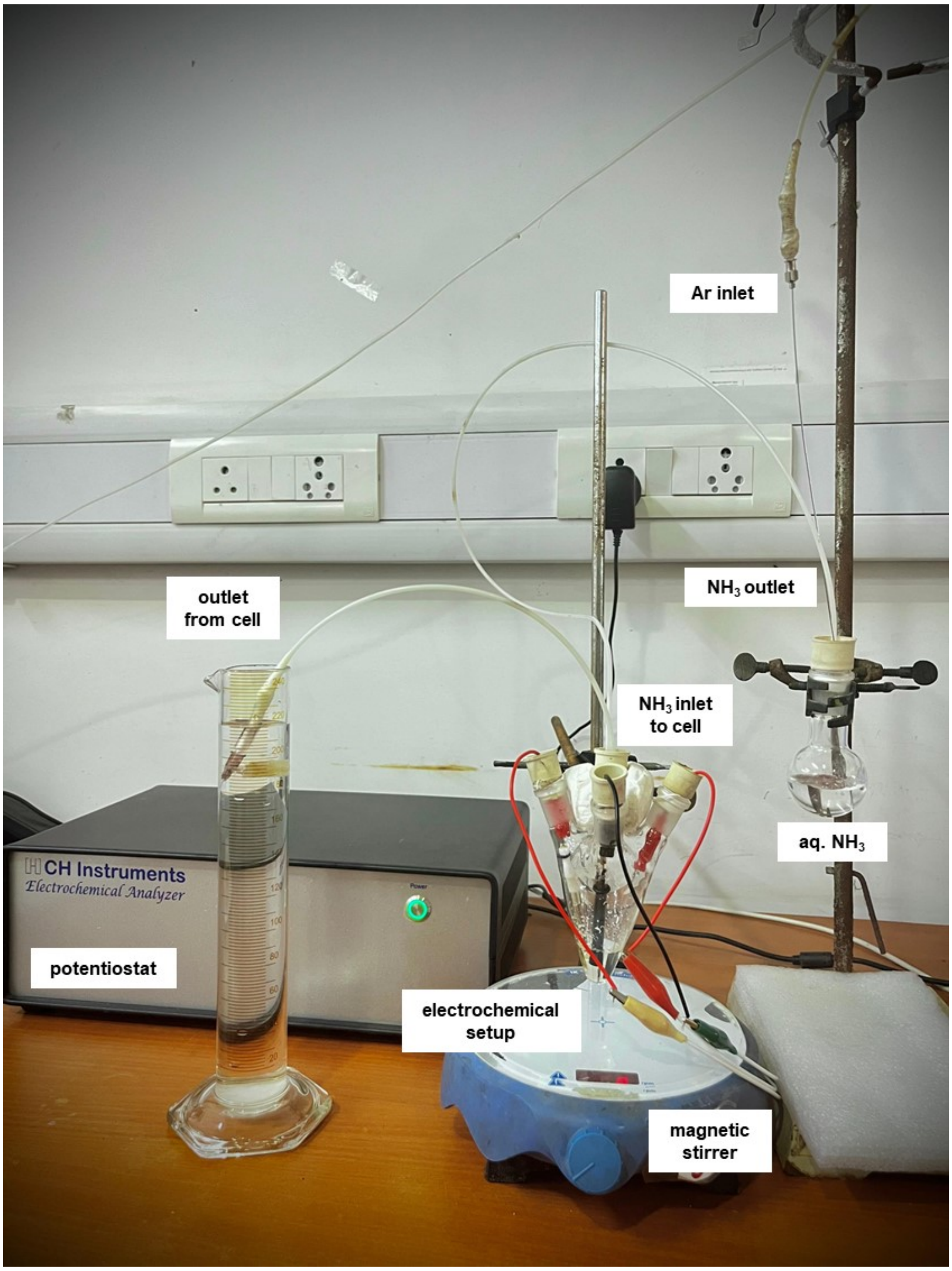

Figure S1. Photograph of the experimental setup.

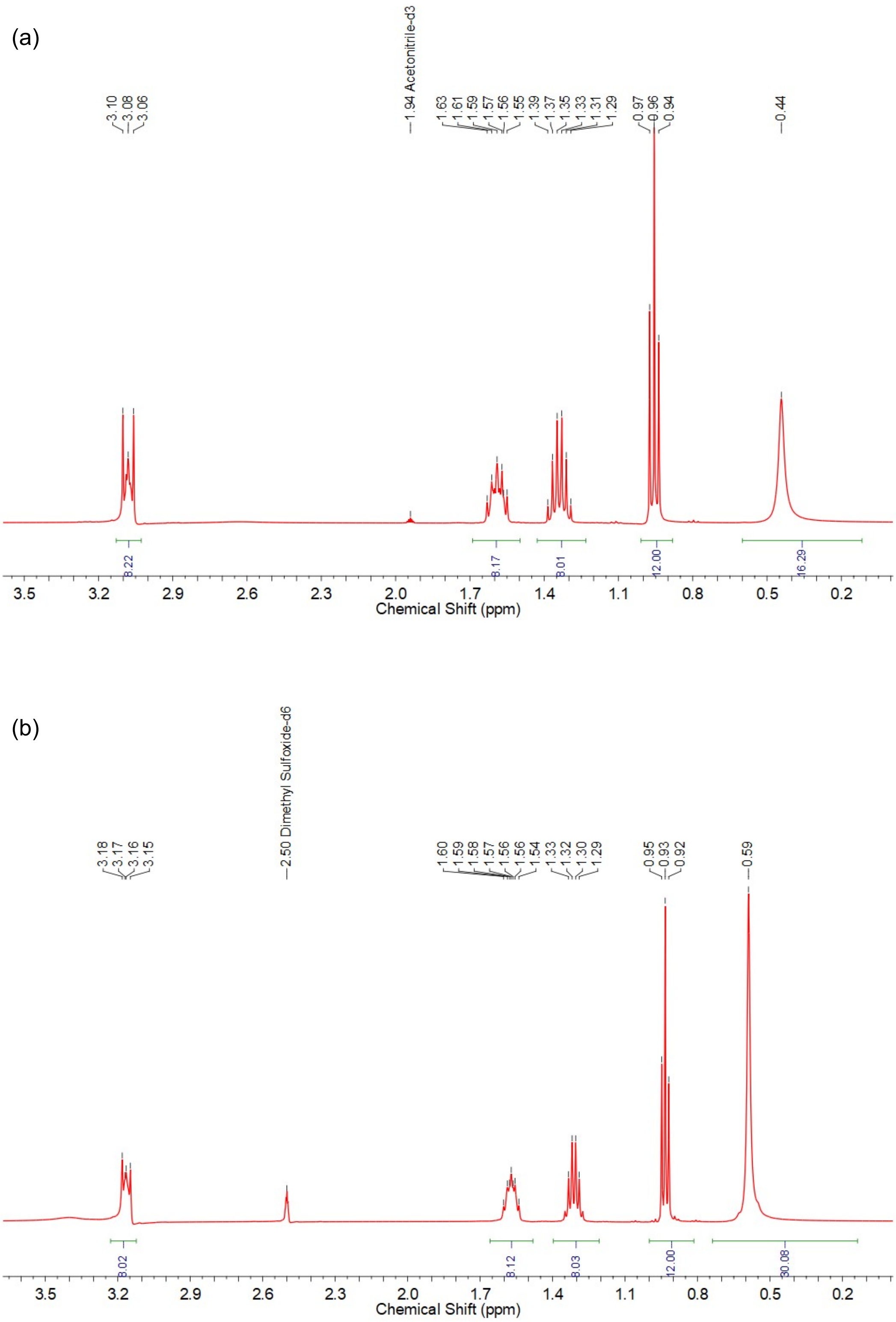

Figure S2. Representative ^{1}H-NMR spectrum of NH_3 saturated (a) CD_3CN and (b) DMSO-d_6, containing 100 mM TBAF (tetrabutylammonium tetrafluoroborate) as internal standard.

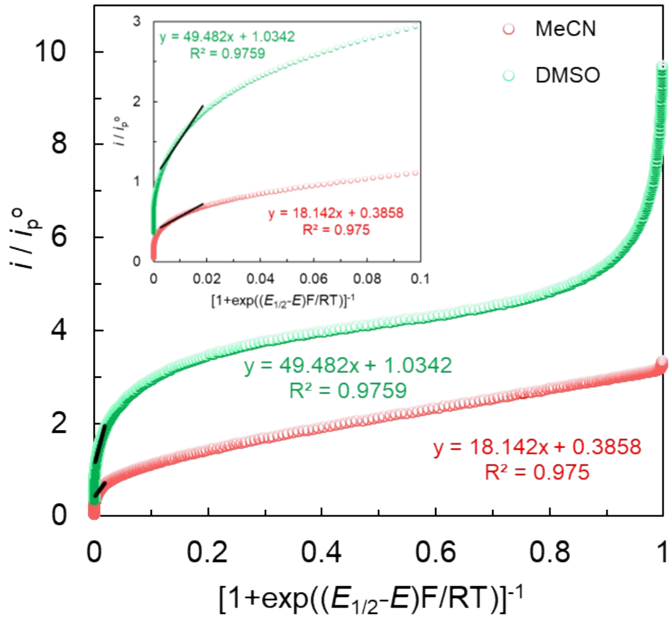

Figure S3. FOWA for mediated AOR in MeCN (red) and DMSO (green) in the range 9 – 15 µA. Experimental conditions: 1 mM Fcpy; 0.5 M NH_3; 100 mM TBAF as supporting electrolyte in the respective solvent; glassy carbon, Pt wire, and Ag/AgCl were used as the working, counter, and reference electrodes, respectively; 298 K; the potential is adjusted with respect to $Fc^{+/0}$.

Table S1. Summary of k_{obs} values determined through FOWA corresponding to MeCN and DMSO solvent systems in different current (*i*) ranges.

FOWA Range (in terms of *i*)	**15 – 25 µA**		**9 – 15 µA**	
	Slope	k_{obs} (s^{-1})	Slope	k_{obs} (s^{-1})
MeCN	3.5	0.3	18.1	7.1
DMSO	16.7	6.0	49.5	52.8

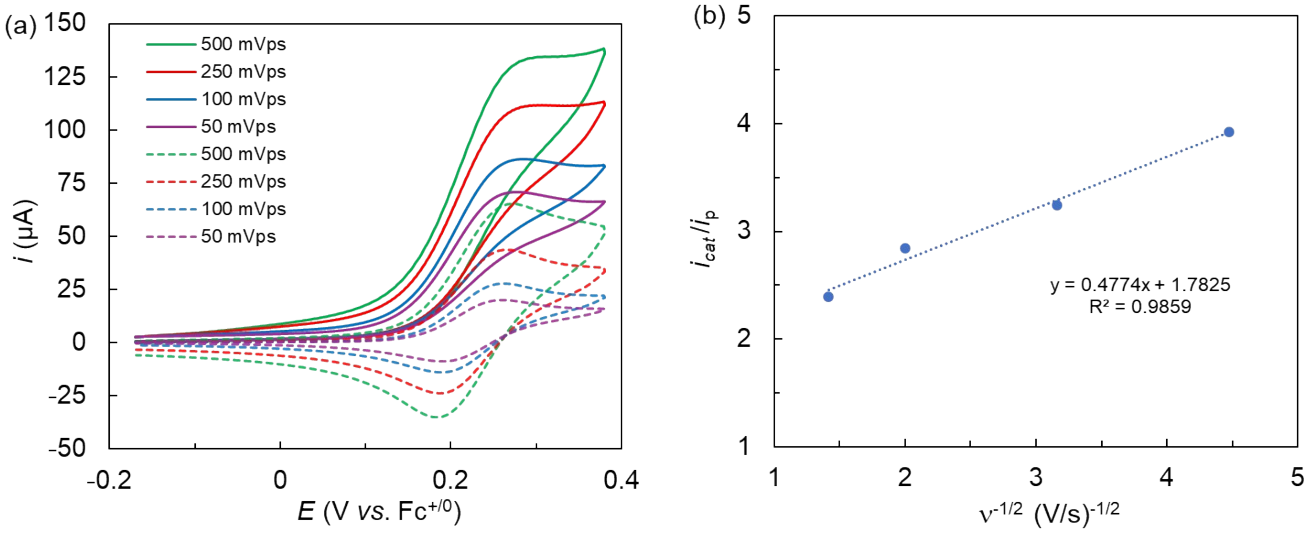

Figure S4. Rate constant (k_{obs}) determination in MeCN for AOR using peak current method: (a) Cyclic voltammograms of the scan-rate dependent Fcpy-mediated AOR (dashed and bold curves represent in the absence and presence of NH_3, respectively) in the range 50-500 mV/s; (b) The corresponding i_{cat}/i_p *vs.* $\nu^{-1/2}$ plot. Experimental conditions: 1 mM Fcpy; 0.5 M NH_3; 100 mM TBAF as supporting electrolyte in MeCN; glassy carbon, Pt wire, and Ag/AgCl were used as the working, counter, and reference electrodes, respectively; 298 K; the potential is adjusted with respect to $Fc^{+/0}$.

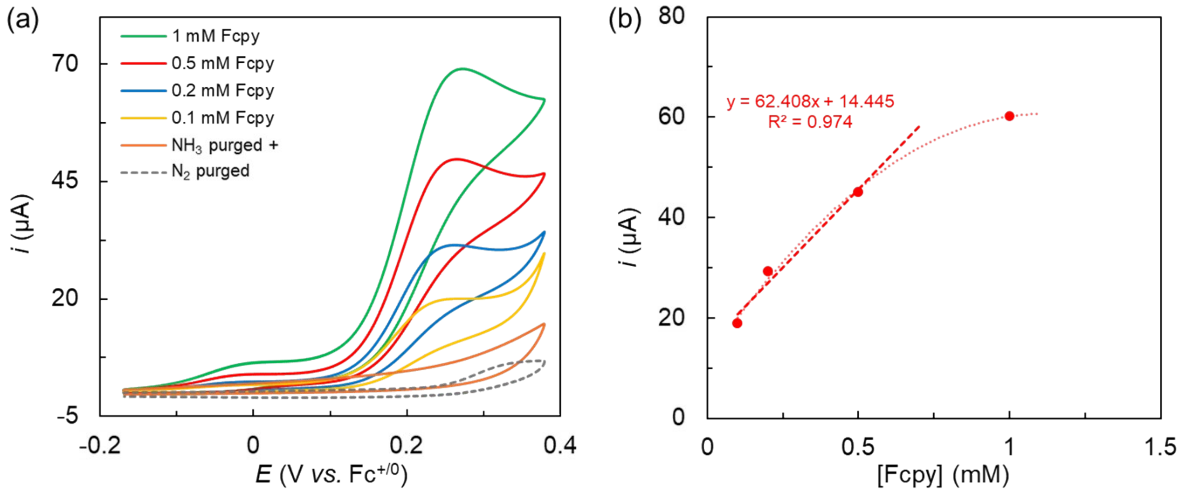

Figure S5. Concentration dependence study of Fcpy (mediator): (a) Cyclic voltammograms of the concentration dependence of mediator (Fcpy) (in the presence of saturated NH_3) for mediated AOR; (b) The corresponding i_{cat} *vs.* concentration plot for Fcpy. Experimental conditions: 100 mM TBAF as supporting electrolyte in acetonitrile; glassy carbon, Pt wire, and Ag/AgCl were used as the working, counter, and reference electrodes, respectively; 298 K; the potential is adjusted with respect to $Fc^{+/0}$.

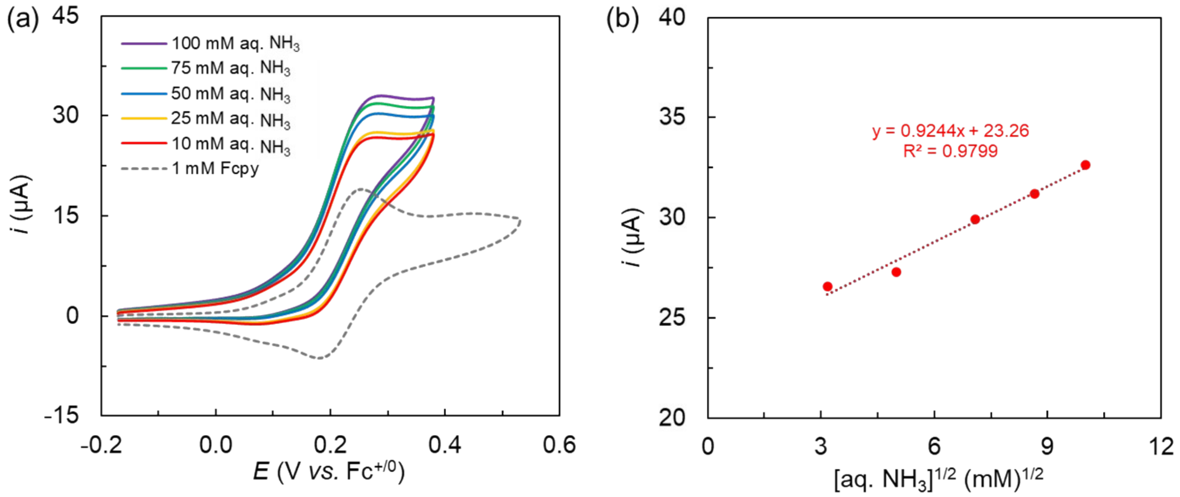

Figure S6. Concentration dependence study of NH_3 (substrate): (a) Cyclic voltammograms of the concentration dependence of aq. NH_3 (in the presence of 1 mM Fcpy) for mediated AOR; (b) The corresponding i_{cat} *vs.* concentration plot for aq. NH_3. Experimental conditions: 100 mM TBAF as supporting electrolyte in acetonitrile; glassy carbon, Pt wire, and Ag/AgCl were used as the working, counter, and reference electrodes, respectively; 298 K; the potential is adjusted with respect to $Fc^{+/0}$.

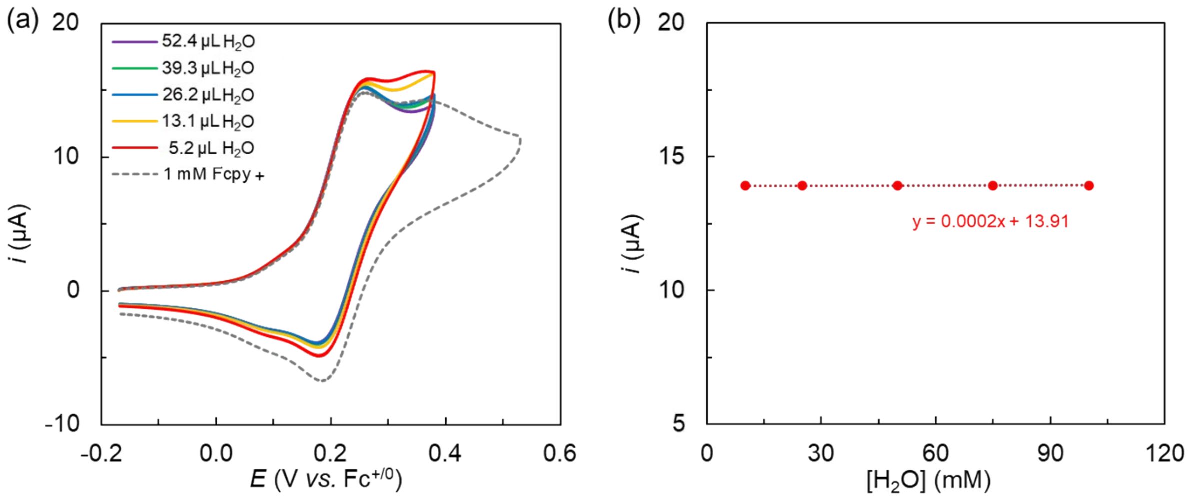

Figure S7. Concentration dependence study of blank H_2O (without ammonia): (a) Cyclic voltammograms of the volume dependence of H_2O (corresponding to the similar amounts taken in [aq. NH_3] dependence in Fig. S4) in the presence of 1 mM Fcpy; (b) The corresponding i_{cat} *vs.* concentration plot for blank H_2O. Experimental conditions: 100 mM TBAF as supporting electrolyte in acetonitrile; glassy carbon, Pt wire, and Ag/AgCl were used as the working, counter, and reference electrodes, respectively; 298 K; the potential is adjusted with respect to $Fc^{+/0}$.

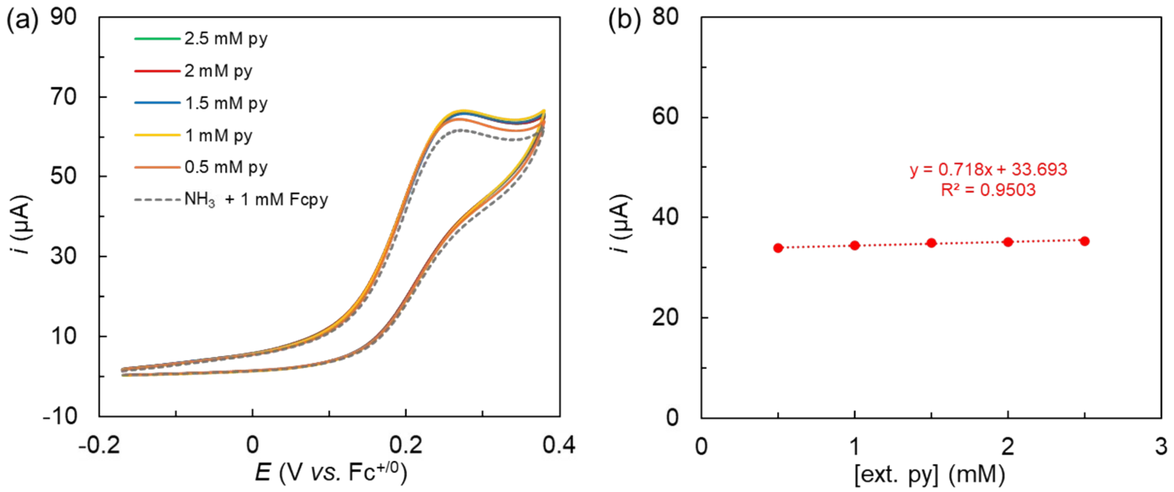

Figure S8. Concentration dependence study of exogenous pyridine (external base): (a) Cyclic voltammograms of the concentration dependence of external pyridine as a base (in the presence of sat. NH_3 and 1 mM Fcpy) for mediated AOR; (b) The corresponding i_{cat} *vs.* concentration plot for external pyridine. Experimental conditions: 100 mM TBAF as supporting electrolyte in acetonitrile; glassy carbon, Pt wire, and Ag/AgCl were used as the working, counter, and reference electrodes, respectively; 298 K; the potential is adjusted with respect to $Fc^{+/0}$.

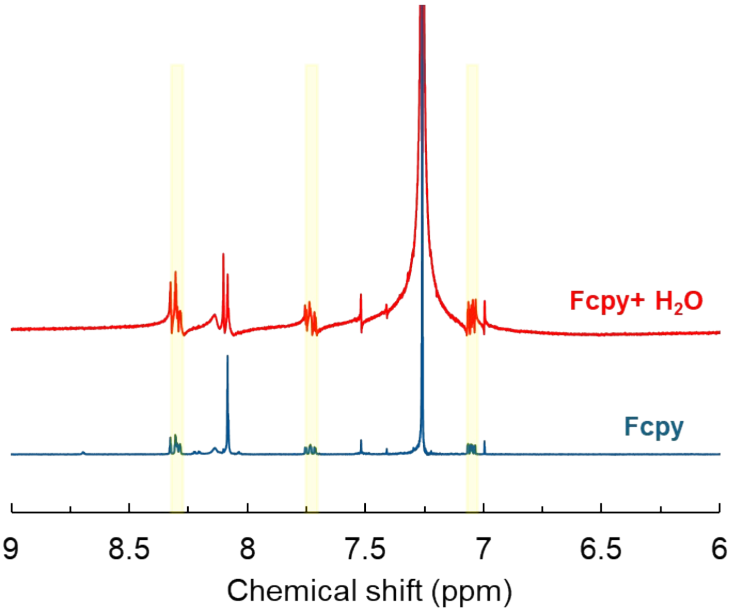

Figure S9. ^{1}H-NMR spectra (500 MHz, 298 K, $CDCl_3$) of Fcpy upon bubbling Ar from water for 1 h.

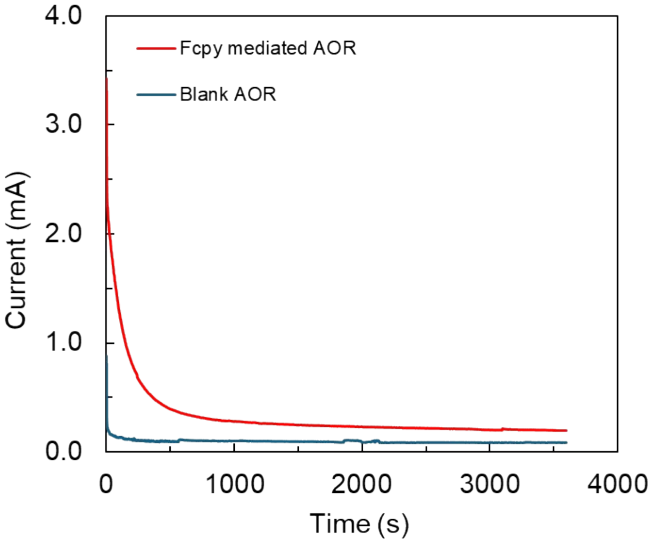

Figure S10. Chronoamperometry results of eAOR: Current *vs.* time profile of the bulk electrolysis at 0.28 V (*vs.* $Fc^{+/0}$) with 1 mM Fcpy (red) and blank (blue) for 1 hour using 1*1 cm^2 carbon-cloth as working electrode. Experimental conditions: 100 mM TBAF as supporting electrolyte in acetonitrile; 298 K.

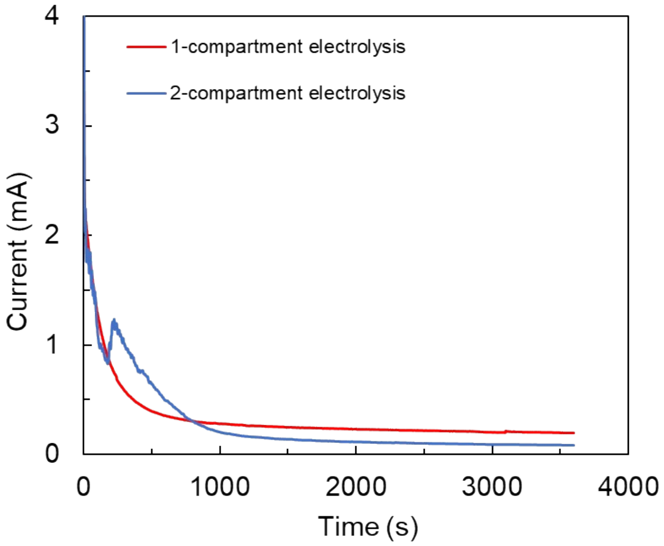

Figure S11. Constant potential electrolysis at 0.28 V (*vs.* $Fc^{+/0}$) for the same duration with 1 mM Fcpy in a single-compartment (red) and a double-compartment cell (blue): (a) Current *vs.* time profile. Experimental conditions: 100 mM TBAF as supporting electrolyte in acetonitrile; 1*1 cm^2 carbon-cloth, Pt wire, and Ag/AgCl were used as the working, counter, and reference electrodes, respectively; 298 K.

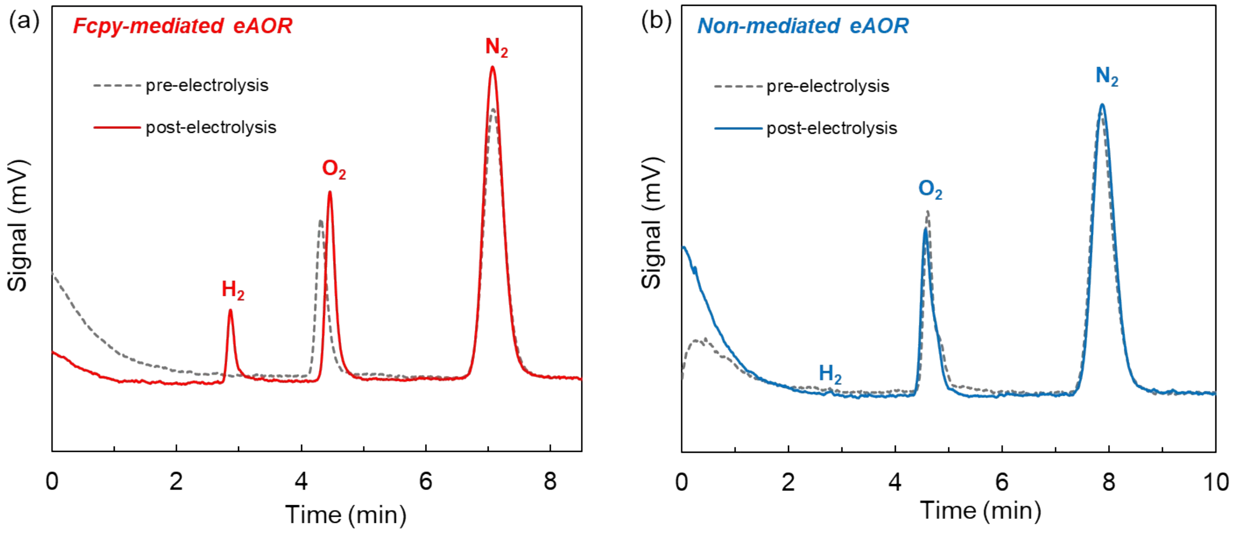

Figure S12. GC Chromatograms of TCD signals from the measured gaseous products in 0.2 mL sample injected from the headspace of the electrolysis cell during: (a) Fcpy-mediated and (b) non-mediated (blank) *e*AOR. The background air was recorded (pre-electrolysis) for the correct quantification of N_2 as shown in the grey dashed line for the respective electrolysis.

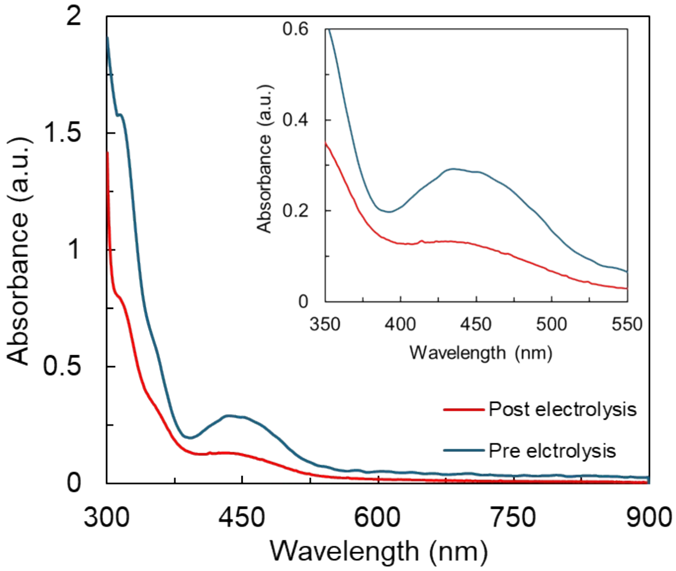

Figure S13. Pre- and post-electrolysis characterization using UV-vis spectra: Fcpy after saturation of NH_3 before electrolysis (blue) and after electrolysis (red).

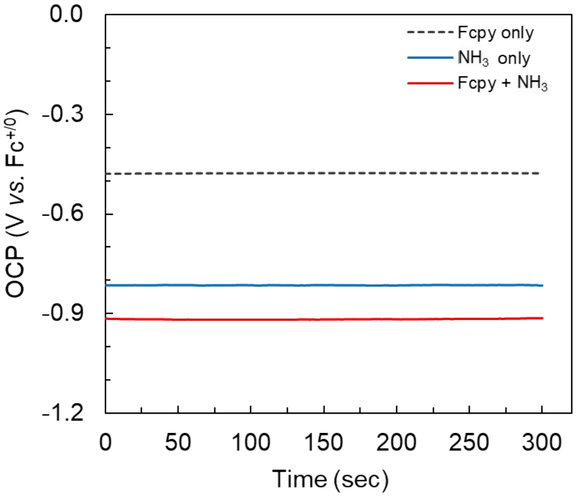

Figure S14. Open-circuit potential (OCP) *vs*. time profile: OCP of Fcpy only (gray dash), NH_3 only (blue), and Fcpy + NH_3 (red) for the duration of 5 minutes with an average of three measurements. Experimental conditions: 100 mM TBAF as supporting electrolyte in acetonitrile; carbon cloth, Pt wire, and Ag/AgCl were used as the working, counter, and reference electrodes, respectively; 298 K; the potential is adjusted with respect to $Fc^{+/0}$.

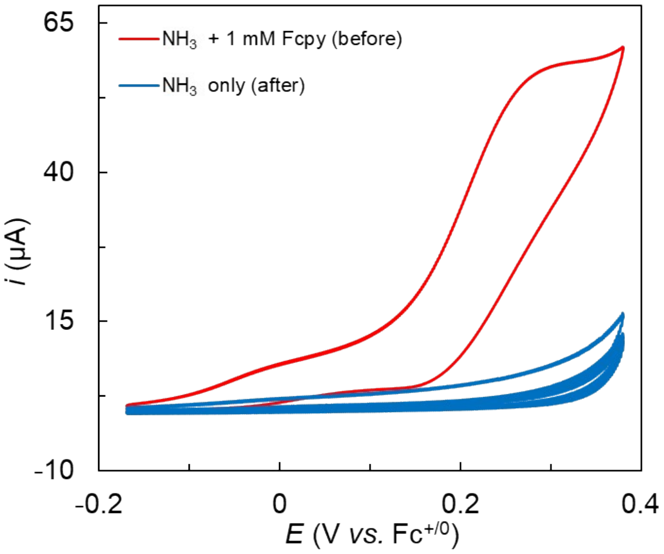

Figure S15. Electrocatalytic performance after the rinse test: CV (1st cycle) of mediated AOR in the presence of 1 mM Fcpy before the rinse test (red) and blank AOR (blue) using the same glassy carbon after rinsing with dry MeCN. Experimental conditions: 100 mM TBAF as supporting electrolyte in acetonitrile; glassy carbon, Pt wire, and Ag/AgCl were used as the working, counter, and reference electrodes, respectively; 298 K; the potential is adjusted with respect to Fc$^{+/0}$.

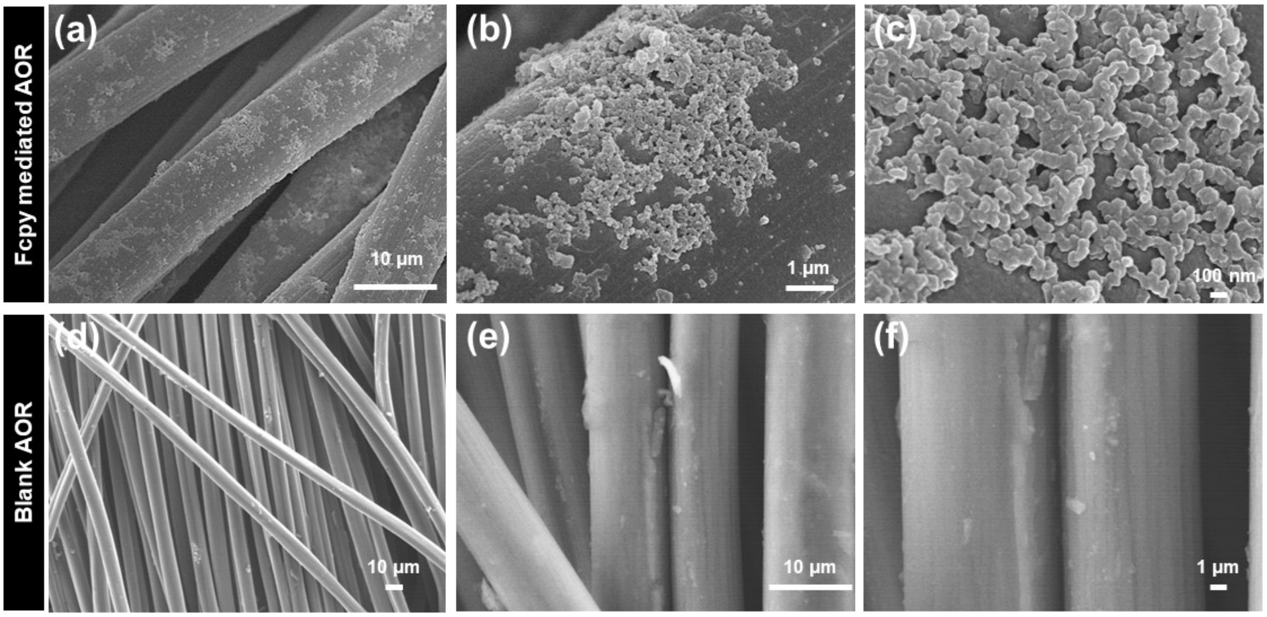

Figure S16. Post-electrolysis characterization using FE-SEM: SEM images (at different magnifications) of rinsed carbon cloth electrode after (upper panel-a,b,c) Fcpy-mediated AOR electrolysis; (lower panel-d, e, f) blank AOR electrolysis.

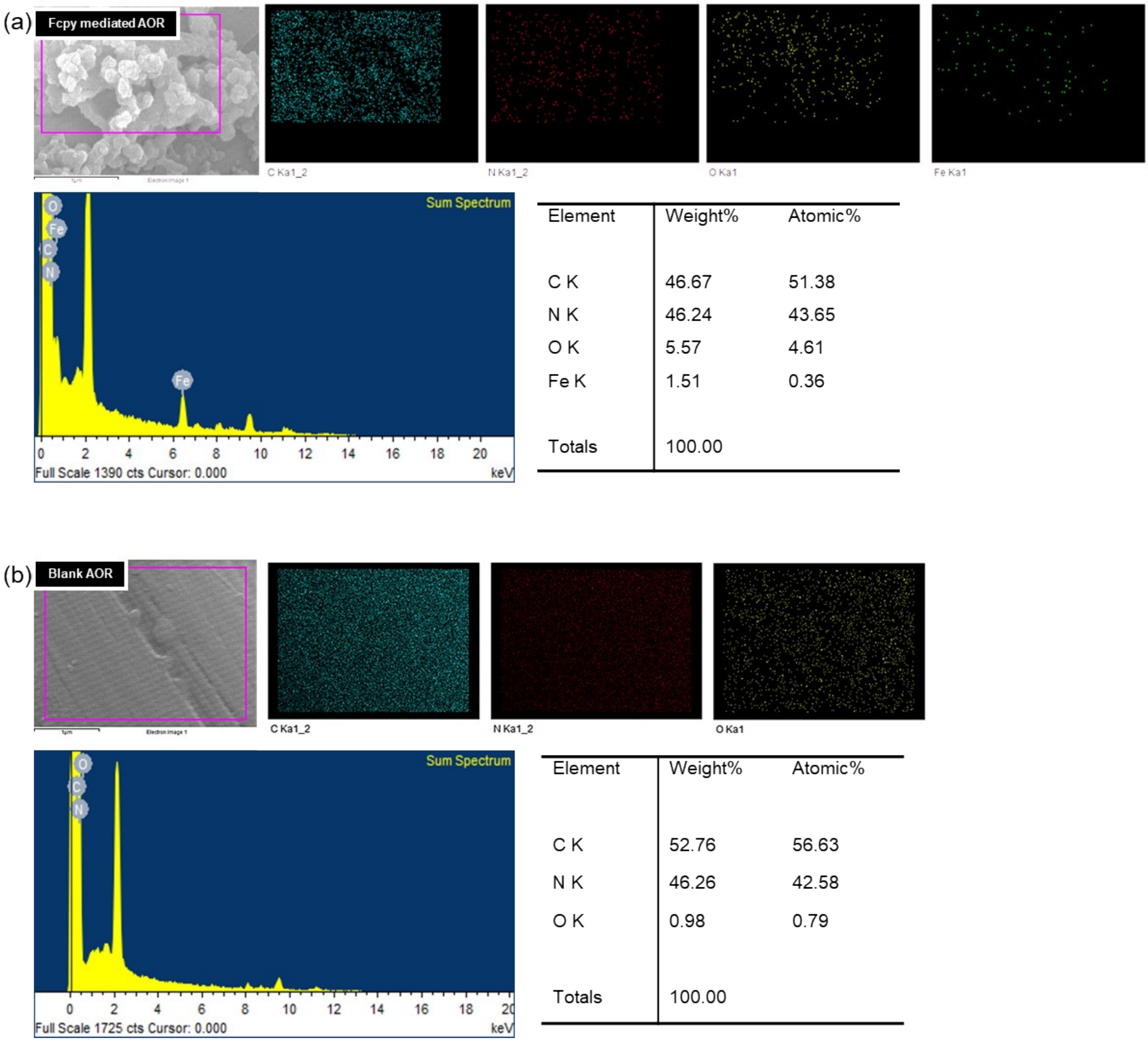

Element	Weight%	Atomic%
C K	46.67	51.38
N K	46.24	43.65
O K	5.57	4.61
Fe K	1.51	0.36
Totals	100.00	

Element	Weight%	Atomic%
C K	52.76	56.63
N K	46.26	42.58
O K	0.98	0.79
Totals	100.00	

Figure S17. Post-electrolysis characterization using EDS: Elemental mapping, EDS spectra, and % composition of rinsed carbon cloth electrode after (upper panel-a) Fcpy-mediated AOR electrolysis; (lower panel-b) blank AOR electrolysis.

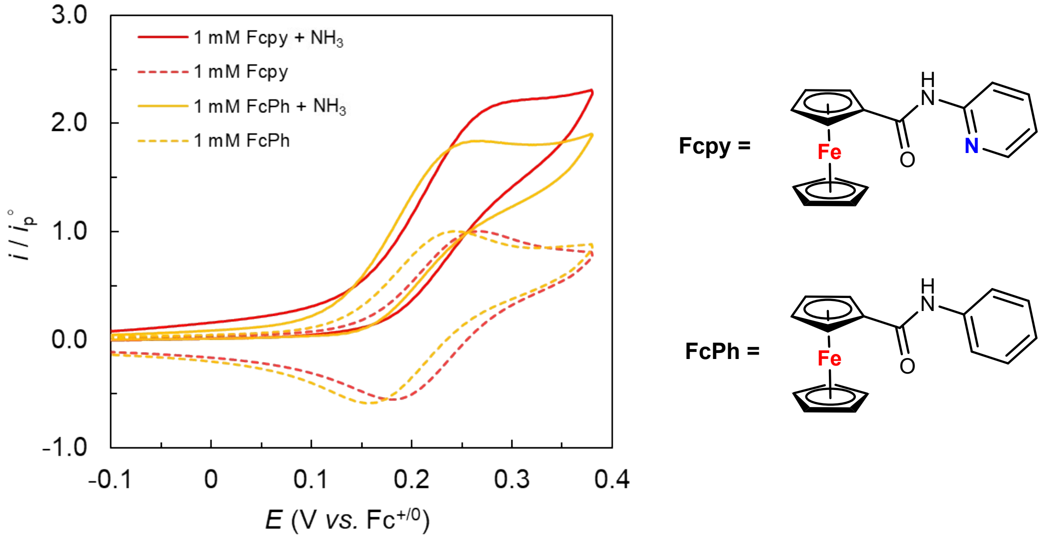

Figure S18. Cyclic voltammograms of Fcpy (*N*-pyridylferrocenocarboxamide)-mediated in red *vs.* FcPh (*N*-phenylferrocenecarboxamide)-mediated AOR in yellow: N_2 purged (dotted) and NH_3 purged (bold) in MeCN. Experimental conditions: 100 mM TBAF as supporting electrolyte in MeCN; glassy carbon, Pt wire, and Ag/AgCl were used as the working, counter, and reference electrodes, respectively; 298 K; 1 mM Mediator; scan rate = 500 mV/s; the potential is adjusted with respect to $Fc^{+/0}$.

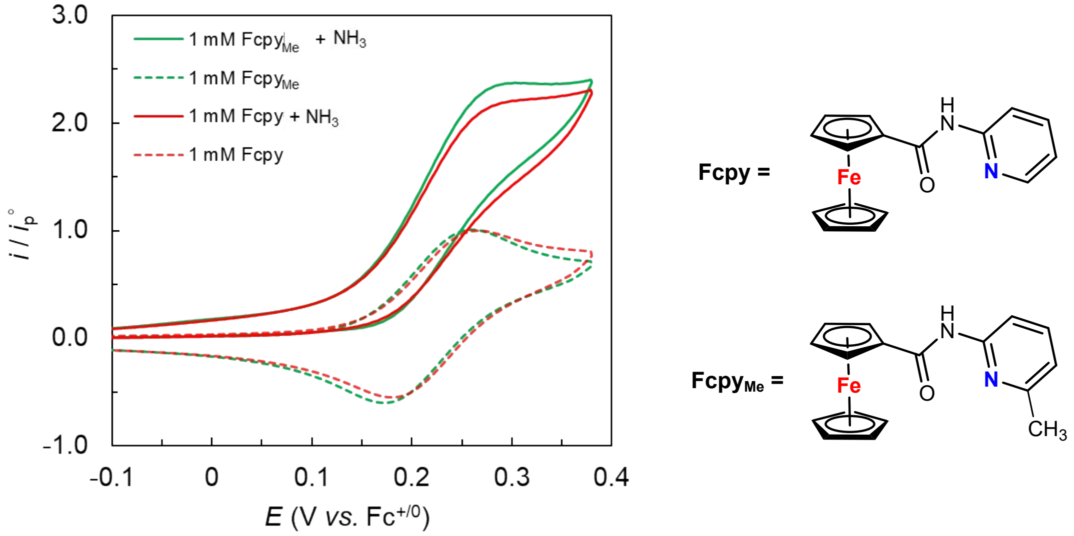

Figure S19. Cyclic voltammograms of Fcpy (*N*-pyridylferrocenocarboxamide)-mediated in red *vs.* FcPh (*N*-phenylferrocenecarboxamide)-mediated AOR in yellow: N_2 purged (dotted) and NH_3 purged (bold) in MeCN. Experimental conditions: 100 mM TBAF as supporting electrolyte in MeCN; glassy carbon, Pt wire, and Ag/AgCl were used as the working, counter, and reference electrodes, respectively; 298 K; 1 mM Mediator; scan rate = 500 mV/s; the potential is adjusted with respect to $Fc^{+/0}$.

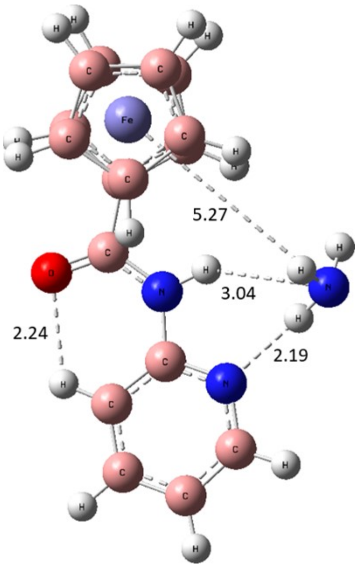

Figure S20. Relevant bond distances in the system having Fc⁺py mediator and ammonia are shown as dotted lines, with the distance unit expressed in angstroms.[13]

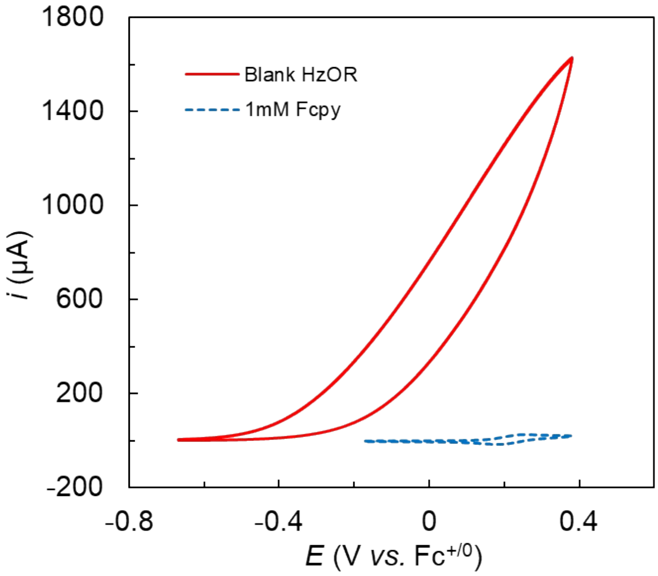

Figure S21. Cyclic voltammograms of non-mediated 100 mM HzOR in red (bold) and 1 mM Fcpy in MeCN. Experimental conditions: 100 mM TBAF as supporting electrolyte in MeCN; glassy carbon, Pt wire, and Ag/AgCl were used as the working, counter, and reference electrodes, respectively; 298 K; the potential is adjusted with respect to Fc$^{+/0}$.

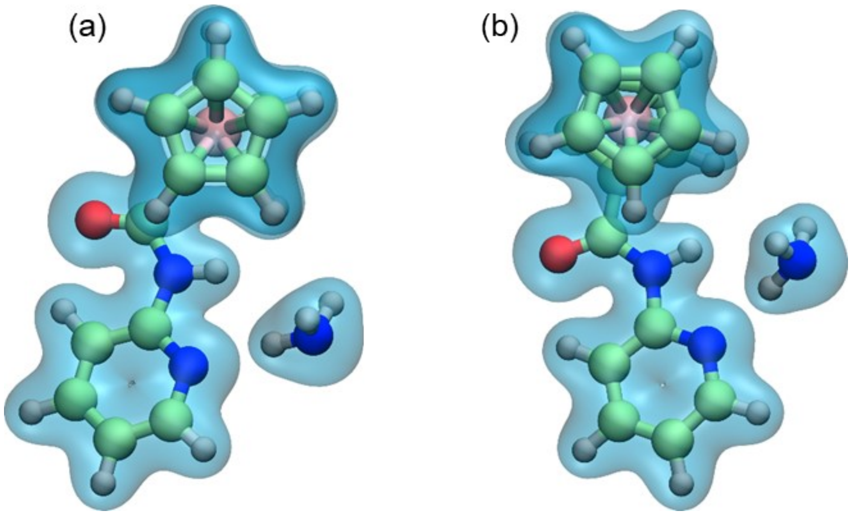

Figure S22. Electron density plot of the catalyst: (a) neutral Fcpy (left), and (b) cationic Fc$^+$py (right), shown at an iso value of 0.025.

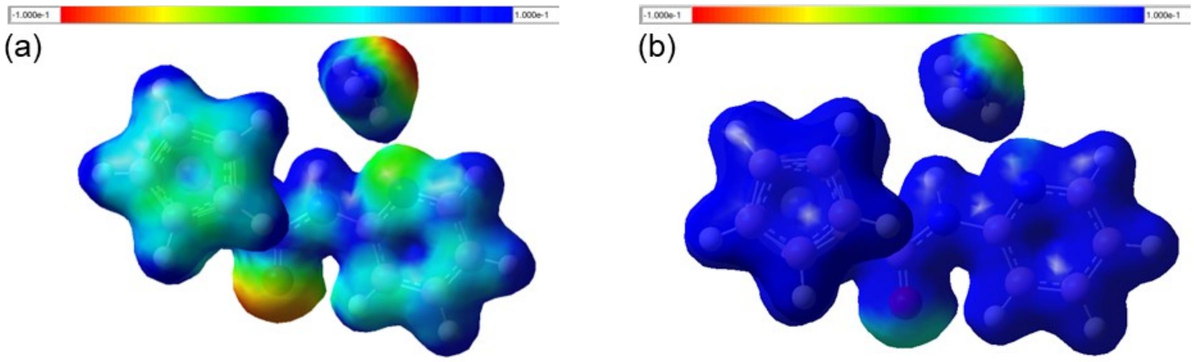

Figure S23. Electron density plot with the mapped electrostatic potential (a) neutral Fcpy (left), and (b) cationic Fc$^+$py (right). The potential changes from -0.1 to +0.1, where blue indicates a donating tendency (positive potential) and red represents an accepting tendency (negative potential).

Table S2. Comparative analysis of this study and previously reported system for *e*AOR (*J.Am.Chem.Soc.* **2025,** *147,* 6514).[4]

Parameters	*J.Am.Chem.Soc.* **2025,** *147,* 6514	***This Work***
Catalyst/Mediator used	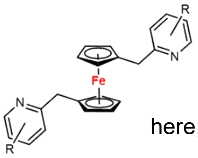 here, R=H	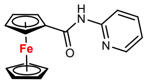
$E_{1/2}$ of mediators (V *vs*. Fc$^{+/0}$)	0.04	0.22
Diffusion coefficient of Mediators (× 10^{-6} cm^{2}s^{-1})	1.54	2.9
Source of NH_3	Anhydrous NH_3 gas	Bubbled aqueous NH_3 solution
[NH_3]	2.4 M in DMSO & 1.3 M in MeCN	1.0 M in DMSO & 0.5 M in MeCN
Overpotential in MeCN (in mV)	820	960
Solvent used for AOR study	DMSO	MeCN
k_{obs} (s^{-1}) using peak current method	0.034 ± 0.002 (DMSO)	0.046 ± 0.002 (MeCN)
KIE (k_{ND3}/k_{NH3})	2.05 (DMSO), experimentally	1.2 (MeCN), computationally
Rate Determining Step (RDS)	PCET	PCET
Rate Law	k[^{py2}Fc][NH_3]	k[Fcpy][NH_3]
% FE (N_2)	76	95
% FE (H_2)	69	87

Supporting Information References

1 T. Gupta, Yati, Sanyam, A. Mondal and B. Mondal, *ACS Catal.*, 2024, **14**, 17690–17698.

2 M. E. Ahmed, M. Raghibi Boroujeni, P. Ghosh, C. Greene, S. Kundu, J. A. Bertke and T. H. Warren, *J. Am. Chem. Soc.*, 2022, **144**, 21136–21145.

3 R. Borougeni, C. Greene, J. A. Bertke and T. H. Warren, *ChemRxiv*, 2019, 1–11.

4 M. E. Ahmed, R. J. Staples, T. R. Cundari and T. H. Warren, *J. Am. Chem. Soc.*, 2025, **147**, 6514–6522.

5 C. Costentin, S. Drouet, M. Robert and J. M. Savéant, *J. Am. Chem. Soc.*, 2012, **134**, 11235–11242.

6 F. Franco, M. F. Pinto, B. Royo and J. Lloret-Fillol, *Angew. Chemie - Int. Ed.*, 2018, **57**, 4603–4606.

7 S. Behera, S. T. Aziz, N. Singla and B. Mondal, *Chem. Commun.*, 2023, **59**, 11528–11531.

8 A. Q. Mir, G. Joshi, P. Ghosh, S. Khandelwal, A. Kar, R. Hegde, S. Khatua and A. Dutta, *ACS Energy Lett.*, 2019, 2428–2435.

9 H. Y. Liu, H. M. C. Lant, C. Decavoli, R. H. Crabtree and G. W. Brudvig, *J. Am. Chem. Soc.*, 2025, **147**, 1624–1630.

10 F. Neese, *WIREs Comput Mol Sci* 2012, 2: 73–78.

11 L. Melander, W. H. Saunders, *Reaction Rates of Isotopic Molecules*, Wiley, New York 1980.

12 J. R. Dunlop, F. P. Tully, *J. Phys. Chem.*, 1993, **97**, 43, 11148–11150.

13 Frisch, M. J., Trucks, G. W., Schlegel, H. B., Scuseria, G. E., Robb, M. A., Cheese-man, J. R., Scalmani, G., Barone, V., Mennucci, B., Petersson, G. A. et al., Gaussian 09, 2009, Revision E.01., Gaussian Inc.: Wallingford CT.